Published online 10 March 2009

Nucleic Acids Research, 2009, Vol. 37, No. 8 ***2723–2736***
doi:10.1093/nar/gkp129

Reconstitution of 'floral quartets' *in vitro* involving class B and class E floral homeotic proteins

Rainer Melzer and Günter Theißen*

Friedrich Schiller University Jena, Department of Genetics, Philosophenweg 12, D-07743 Jena, Germany

Received October 31, 2008; Revised February 13, 2009; Accepted February 16, 2009

ABSTRACT

Homeotic MADS box genes encoding transcription factors specify the identity of floral organs by interacting in a combinatorial way. The 'floral quartet model', published several years ago, pulled together several lines of evidence suggesting that floral homeotic proteins bind as tetramers to two separated DNA sequence elements termed 'CArG boxes' by looping the intervening DNA. However, experimental support for 'floral quartet' formation remains scarce. Recently, we have shown that the class E floral homeotic protein SEPALLATA3 (SEP3) is sufficient to loop DNA in floral-quartet-like complexes *in vitro*. Here, we demonstrate that the class B floral homeotic proteins APETALA3 (AP3) and PISTILLATA (PI) do only weakly, at best, form floral-quartet-like structures on their own. However, they can be incorporated into such complexes together with SEP3. The subdomain K3 of SEP3 is of critical importance for the DNA-bound heterotetramers to be formed and is capable to mediate floral quartet formation even in the sequence context of AP3 and PI. Evidence is presented suggesting that complexes composed of SEP3, AP3 and PI form preferentially over other possible complexes. Based on these findings we propose a mechanism of how target gene specificity might be achieved at the level of floral quartet stability.

INTRODUCTION

One central question of developmental biology is how pattern formation is accomplished. For obtaining detailed answers, the angiosperm flower is one of the best-understood genetic model systems. Dozens of genes have been identified that constitute an intricate network controlling flower development (1–4). Of special interest are the genes that determine floral organ identity. A standard angiosperm flower is composed of four different organs, sepals, petals, stamens and carpels; the latter two being the male and female reproductive organs, respectively. In *Arabidopsis thaliana*, mutant analysis has shown that the identity of these organs is specified by only a few genes that (with one exception) encode transcription factors of the MADS domain family. These genes have been grouped into the four functional classes A, B, C and E of floral homeotic genes (5–8). The combinatorial interaction between genes of these classes is proposed to confer the identity of the different floral organs. For example, in wild type *Arabidopsis* plants class A, B and E floral homeotic genes together specify petal development, whereas class B, C and E genes function in determining stamen identity. In *Arabidopsis*, class A genes are *APETALA1* (*AP1*) and *APETALA2* (*AP2*) (the only non-MADS box floral homeotic gene), class B genes are *APETALA3* (*AP3*) and *PISTILLATA* (*PI*), the only class C gene is *AGAMOUS* (*AG*) and the class E genes are the redundantly acting genes *SEPALLATA1 (SEP1)*, *SEP2*, *SEP3* and *SEP4* (2,6–8).

How the genetic interactions of floral homeotic genes are realized at the molecular level is not well understood. According to the 'floral quartet model', two dimers of floral homeotic proteins bind to two nearby *cis*-regulatory DNA elements and interact with each other by looping the intervening DNA (8,9). Thus, the quartet model maintains that the differential formation of DNA bound tetrameric transcription factor complexes controls floral organ identity. Specifically, a complex of one class A, two class B and one class E protein has been hypothesized to determine petal identity, whereas a complex of two class B, one class C and one class E protein is postulated to function in stamen specification, likely because different tetrameric protein complexes bind to the regulatory regions of different (petal or stamen specific, respectively) target genes (8,9). How target gene specificity is achieved has remained unknown, however, partly because all dimers of MADS domain proteins appear to bind to very similar DNA sequences termed CArG boxes (for 'CC-Arich-GG', consensus sequence 5′-CC(A/T)$_6$GG-3′) (10,11).

Despite its plausibility, experimental support for the 'floral quartet model' is still scarce. Yeast three-hybrid experiments and electrophoretic mobility shift assays

*To whom correspondence should be addressed. Tel: +49 3641 949 550; Fax: +49 3641 949 552; Email: guenter.theissen@uni-jena.de

(EMSAs) indicated that the *Antirrhinum majus* class B floral homeotic proteins DEFICIENS (DEF) and GLOBOSA (GLO) form higher-order complexes together with the class A-related protein SQUAMOSA (SQUA) (12). Furthermore, yeast three- and four-hybrid experiments indicated that SEP3 or AP1 together with AP3 and PI as well as SEP3 and AG together with AP3 and PI form higher order complexes (13). In addition, ectopic expression of AP3 and PI together with SEP3 and/or AP1 in *Arabidopsis* leads to the development of petals from primordia that would normally develop into vegetative leaves (13,14). Notably, the ectopic expression of SEP3, AP3 and PI is sufficient to induce this organ transformation, ectopic expression of AP1 is not required (13), suggesting that SEP3, AP3 and PI represent a minimal set of master control elements governing petal identity. This is in line with data indicating that the main function of *AP1* is in specifying floral meristem identity and that defects observed in floral organ development in *ap1* mutants are by-products of defects in floral meristem specification (see refs 15,16 and references therein).

Similarly, simultaneous ectopic expression of SEP3, AP3, PI and AG leads to the conversion of cauline leaf primordia into primordia that develop into stamens (13). These data suggest, but by no means conclusively demonstrate, that floral homeotic proteins form floral quartets *in planta*. Alternatively, different combinations of independently DNA binding dimers, or ternary or quaternary complexes binding to only one *cis*-regulatory element, may control the activity of target genes (17).

The structure and the protein–protein interactions of floral homeotic MADS domain transcription factors have been the subject of numerous research projects (12,18,19,20). All floral homeotic MADS domain proteins have a modular structure composed of the MADS, Intervening, Keratin-like and C terminal domain which classifies them as MIKC type MADS domain proteins (21–23). The most highly conserved domain is the MADS domain that is responsible for specifically binding to CArG boxes (24). The I domain has been implicated in conferring functional specificity (25,26) and, together with the MADS domain, in the formation of DNA-binding dimers. The K domain is the second most conserved domain. It is predicted to form three amphipathic alpha helices K1, K2 and K3 that are involved in protein–protein interactions (18,19). Finally, the C terminal domain is the least conserved region, which has been implicated to function in transcriptional activation and mediating protein–protein interactions in some cases (13,27–29). So far, it is not clear which domains are essential for higher-order complex formation of MADS domain transcription factors. Some reports indicate that the C terminal domain plays an important role (12,13) while others ascribe a more prominent function to the K domain (19). It is also unclear whether regions for dimerization and tetramerization can be experimentally separated.

Furthermore, whether tetramer formation is an intrinsic feature of some or even all MIKC type proteins, or depends on specific combinations of different proteins, remains largely unknown. The same is true for the extent to which the formation of tetrameric complexes depends on DNA binding.

Using suitably designed DNA probes, here we provide biochemical evidence suggesting that heterodimers of the class B floral homeotic proteins AP3 and PI do form floral-quartet-like complexes on their own only weakly, at best, but that they can be more efficiently incorporated into such structures together with homodimers of SEP3. Domain-deletion and domain-swapping experiments indicate that the subdomain K3 of SEP3 is involved in tetramer formation and is sufficient to confer the ability of tetramer formation to AP3 and PI. We also present evidence indicating that complexes composed of SEP3, AP3 and PI form preferentially over SEP3 homotetramers, suggesting as to how at different developmental stages different target genes can be activated.

MATERIALS AND METHODS

In vitro translation templates and DNA-binding site probes

The constructs used to produce SEP3 (and the truncated versions), AP3 and PI proteins by *in vitro* translation have been described previously (25,30,31). SEP3 was produced either from vectors pSPUTK or pTNT. For construction of the chimeric AP3~SEP3 template, a region covering the MADS box to the K2 box of AP3 cDNA was amplified by PCR. The respective PCR product was ligated to a PCR fragment covering the K3 box of SEP3. In a second round of PCR, the desired products were amplified with primers binding to the beginning of the MADS box of AP3 and to the end of the K3 box of SEP3. The chimeric PI~SEP3 template was constructed accordingly. These chimeric constructs were cloned into pTNT using EcoRI and SalI recognition sites. Primers used for amplification are listed in Supplementary Table 1.

Preparation of DNA-binding site probes for EMSA and DNase I footprint analyses was initiated by cloning double-stranded oligonucleotides (named I, II and III) into a plasmid vector. Sequences of the oligonucleotides are shown in Figure 1.

Oligonucleotide I contains a CArG box (henceforth termed '*AG*-derived CArG box') and some surrounding base pairs derived from the regulatory intron of *AG* (31). Oligonucleotide II has the same base composition as oligonucleotide I but a randomized order of nucleotides (30). Oligonucleotide III carries a CArG box-like sequence and some surrounding base pairs derived from the promoter of the *GLO* gene from *Antirrhinum majus* (32). Preparation of probes A, B and C and of the probes in which the phasing between the *AG*-derived CArG boxes was varied has been described previously (30). Briefly, for preparation of probe A, oligunucleotide I was cloned into both, the SalI and EcoRV site of pBluescript II SK (+). This probe thus contained two copies of the *AG*-derived CArG box that are spaced by 63 bp (measured from centre to centre of the CArG boxes). Probe B contained oligonucleotide I cloned into the SalI site and oligonucleotide II cloned into the EcoRV site. In probe C, oligonucleotide I was cloned into the EcoRV site and oligonucleotide II into the SalI site. Thus, probes B and C contain only

one *AG*-derived CArG box. Probe D was constructed by cloning oligonucleotide II into both, the SalI and EcoRV site. This probe was used to test for DNA-sequence specificity of protein binding. Probe E was constructed by cloning oligonucleotide I into the SalI site and oligonucleotide III into the EcoRV site. In this probe, the *AG*-derived CArG box and the CArG box-like sequence derived from the *GLO* promoter are spaced by 63 bp (measured from centre to centre of the boxes). Probe F was prepared by cloning oligonucleotide II into the SalI site and oligonucleotide III into the EcoRV site. Probes are shown schematically in Figure 1.

After cloning, the probes were excised from the plasmids using XbaI and XhoI recognition sites. For the experiment shown in Figure 3B, the probe was excised from the plasmid using EcoRI and XhoI recognition sites. Radioactive labelling was done with T4 polynucleotide kinase or Klenow enzyme. The sequences of the oligonucleotides and the probes are listed in Supplementary Table 2.

In vitro translation, electrophoretic mobility shift assays and DNase I footprint assays

In vitro translation, protein–DNA incubation and electrophoretic mobility shift assays were essentially done as described (30). Protein–DNA incubation was usually for at least 5 h on ice. Protein–DNA incubation prior to DNase I footprint assays and for the experiment shown in Figure 3B was for at least 90 min on ice. In some experiments, ^{35}S methionine was used for radioactive labelling of proteins. Concentration of the DNA probes was usually $\leq$0.1 nM. For EMSAs shown in Figure 3B, concentration of labelled DNA was about 2 nM. When unlabelled DNA was used as probes, concentration was about 10 nM.

Gel run was performed at room temperature, except for the gel shown in Figure 3C that was run at 4°C. When proteins were labelled with ^{35}S methionine, the gel was usually fixed after gel run for 15 min or longer in 50% methanol, 10% acetic acid and 40% distilled water before gel drying. The signals were analysed by autoradiography or phosphorimaging.

For DNase I footprint analyses, probe A was used. The XhoI digested end of the DNA was 5′-labelled with T4 polynucleotide kinase. DNase I (50 U/μl; Fermentas, St. Leon-Rot; Germany) was diluted to 5 U/μl with a buffer containing 9 mM HEPES, pH 7.2, 30 mM $MgCl_2$, 5 mM $CaCl_2$ and 0.1 mg/ml BSA. Footprint analyses were generally done as described (30), except that other combinations of MADS domain proteins were used.

Calculation of co-operativity constants

Co-operative binding was determined as described (30), using published equations (33,34). As the exact protein concentration is not known, the K_{d1}/K_{d2} ratios shown in Figure 2C and D assume that the concentration of protein dimers increases linearly with the amount of *in vitro* translation mixture added. For comparison, we also calculated K_{d1}/K_{d2} ratios by assuming that the concentration of protein monomers rather than that of dimers increases linearly with the amount of *in vitro* translation mixture added (30). This yielded K_{d1}/K_{d2} ratios of 1.35 ($\pm$ 0.19) and 0.96 ($\pm$ 0.11) (standard errors in brackets) for a probe with the *AG*-derived CArG boxes spaced by 6 and 6.5 helical turns, respectively, thus also indicating that AP3-PI heterodimers do not or only weakly bind co-operatively to DNA.

Modelling a floral quartet

For constructing a model of floral quartets, the DNA sequence between the XhoI and XbaI sites of probe A was used. First, a pdb file of a standard B DNA with this DNA sequence was obtained using the 'fiber' program implemented in 3DNA (35). The base pair geometry of this DNA was analysed with the 'analyse' program of 3DNA. The resulting 'bp_step.par' file was opened in MSExcel and helical parameters were modified manually as follows. The helical twist was changed to the more typical average value of 34.29° for DNA in solution (i.e. 10.5 bp per helical turn). Roll angles were modified by multiplying roll angles of the original standard B DNA values (between 1.70° and 1.72°) with the fold change of sensitivity to DNase I digestion obtained from the DNase I footprint data. Fold change for every band was expressed by the quotient $\frac{\text{intensity of bound DNA}}{\text{intensity of free DNA}}$ (intensity was obtained from integrating the area below the signals of the respective bands in a phosphorimager analysis) or, in case this was below 1, by the negative inverse value. Corrections for variations in the amount of DNA loaded were done similar as described in ref. 36 by using invariable bands as internal standards. Fold change used for construction of the model was obtained from the mean of two DNase I footprint experiments. Only roll angles of base pairs between the two CArG boxes and more than 11 bases apart from the CArG boxes have been modified to avoid interference with changes in sensitivity caused by direct protection of the MADS domain proteins. The DNA structure was then reconstructed using the 'rebuild' program of 3DNA, yielding a pdb file that was used to create a picture with Protein Explorer 2.80 (37) that is shown in Figure 6A.

To plot proteins on this DNA structure, the base pair geometry of the CArG box bound to SERUM RESPONSE FACTOR (SRF) (38) was obtained using the 'analyse' program of 3DNA. The original CArG box sequences (plus 1 nt flanking on either side of the CArG boxes) of the previously modified DNA were then replaced manually by the CArG box (plus 1 nt flanking on either side of the CArG boxes) of the crystallized SRF-CArG complex in the respective .par file. The DNA structure was reconstructed using the 'rebuild' command of 3DNA. This yielded a DNA structure similar to the one shown in Figure 6A, but carrying the bent CArG boxes from the SRF-CArG complex. This was done to facilitate not only plotting of the SRF complex on the DNA but also because floral homeotic proteins also bend DNA (although probably to a different degree) (30,39,40). The CArG box bound SRF was plotted manually on this DNA using Swiss pdb viewer (ref. 41; http://www.expasy.org/spdbv/) by aligning the CArG boxes of the modified DNA fragment with those

of the SRF–CArG complex. Amino acids from position 201 on (which do not belong to the MADS domain) were deleted with the Swiss pdb viewer. A picture of the obtained structure was created with Protein Explorer 2.80 (37). Possible positions of the I and K domain were plotted on this picture, yielding the model shown in Figure 6B.

RESULTS

Two AP3-PI heterodimers do barely form tetrameric complexes

Recently, it was shown that SEP3 binds as a homodimer to a DNA probe carrying one CArG box, and that four SEP3 proteins bind to a DNA probe carrying two CArG boxes (30). The different protein–DNA complexes can be distinguished and identified by their characteristic gel electrophoretic mobilities (30). AP3-PI proteins form complexes of similar mobility to the ones observed for SEP3 when binding to probes containing one or two CArG boxes, respectively (Figure 2A, compare lanes 2 and 5, 3 and 6). As AP3 and PI are well known to bind as an obligate heterodimer to CArG box sequences (25,42) this indicates that one heterodimer composed of AP3 and PI binds to a DNA probe containing one CArG box and that two heterodimers (or one tetramer) bind to a DNA fragment carrying two CArG boxes. To determine whether indeed one tetramer rather than two individual dimers of AP3-PI bind to a probe containing two CArG boxes (Figure 2B), we took advantage of the fact that tetramerization via DNA looping is often accompanied by co-operative DNA binding (43). Co-operative binding was studied by adding increasing amounts of *in vitro* translated AP3-PI proteins to a DNA fragment (probe A in Figure 1) carrying two *AG*-derived CArG boxes spaced by six helical turns (63 bp; assuming 10.5 bp per turn) and by quantitative analysis of the resulting band pattern. The analysis revealed that the fraction of the complex corresponding to one dimer bound to the DNA fragment increases up to around 40% of the total signal per lane (Figure 2C). This indicates that the affinity of an AP3-PI dimer to a CArG box is only weakly increased when another AP3-PI dimer is bound already to a neighbouring CArG box.

Another well-known feature of proteins inducing looping upon DNA binding is stereospecificity in DNA binding. Binding sites positioned on the same side of the DNA helix are assumed to corroborate looping more easily compared to sites lying on opposite sides of the DNA (44,45). Using a fragment on which the *AG*-derived CArG boxes were spaced by 6.5 helical turns (68 bp) and thus were assumed to be positioned on opposite sites of the DNA, did only slightly alter the ratio of the dissociation constants for binding of the first and second AP3-PI heterodimer, respectively (Figure 2D). Thus co-operative binding and stereospecificity in binding were hardly detectable for AP3-PI proteins. We conclude that the majority of the complexes of low mobility observed in Figures 2C and D (marked with '4', indicating the number of proteins involved) result from the independent binding of two AP3-PI heterodimers to the two CArG boxes. However, the slight apparent co-operativity and phase dependence of AP3-PI binding observed in our experiments suggest that a weak tendency towards DNA bound tetramer formation may exist.

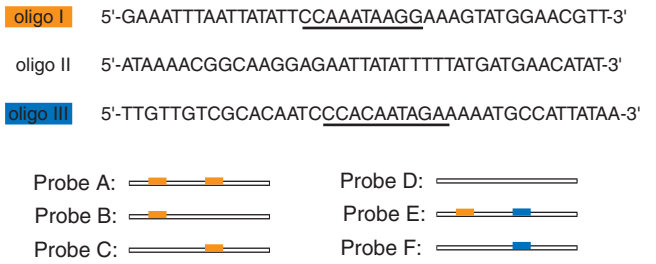

Figure 1. Sequences of the oligonucleotides ('oligo I', 'oligo II' and 'oligo III') used to construct the different DNA probes. The CArG box and a CArG box-like sequence are underlined. DNA probes and the approximate position of the oligonucleotides are depicted schematically. See Supplementary Table 2 for the complete sequences of the probes.

SEP3 can integrate AP3-PI into floral-quartet-like complexes

We next tested whether AP3 and PI can be integrated into a tetrameric protein complex together with SEP3. Such a complex would be similar to a floral quartet that is predicted to specify petal identity (8,9,13). SEP3 alone binds as a dimer to a DNA fragment carrying one CArG box (Figure 3A, lane 3). However, using a fragment carrying two CArG boxes spaced by six helical turns (probe A), a second complex of slower mobility is observed (Figure 3A, lane 4) which contains four molecules of SEP3 bound to DNA (30). Formation of this complex of slower mobility is stereospecific, being stronger when the two CArG boxes are spaced by an integral number of helical turns and weaker when the CArG boxes are separated by a non-integral number of helical turns (Figure 3A). These and other data suggest that this complex of low mobility most likely represents a SEP3 homotetramer bound to DNA (30). However, when SEP3, AP3 and PI were incubated with a probe carrying two CArG boxes (probe A), a band representing a complex with slightly higher mobility than that containing the SEP3 homotetramer was observed (Figure 3B, compare lanes 2 and 6, where the critical band is marked with '4#'). The mobility of this complex was very similar to that consisting of two AP3-PI heterodimers bound to DNA (Figure 3B, lane 4, band 4). However, when SEP3 was added together with AP3-PI to the DNA probe, the respective signal appeared to be stronger compared to an incubation of AP3-PI alone with DNA (Figure 3B, consider lanes 4 and 6). This suggests that a complex has formed in which SEP3 and AP3-PI are bound to the same DNA fragment. We performed differential radioactive labelling of the proteins to test this hypothesis. Indeed, the majority of AP3-PI migrated in a band of slow mobility (band 4#) when SEP3 was present, but not when AP3-PI was applied without SEP3 (Figure 3B, compare lanes 5 and 9). Also, SEP3 migrated

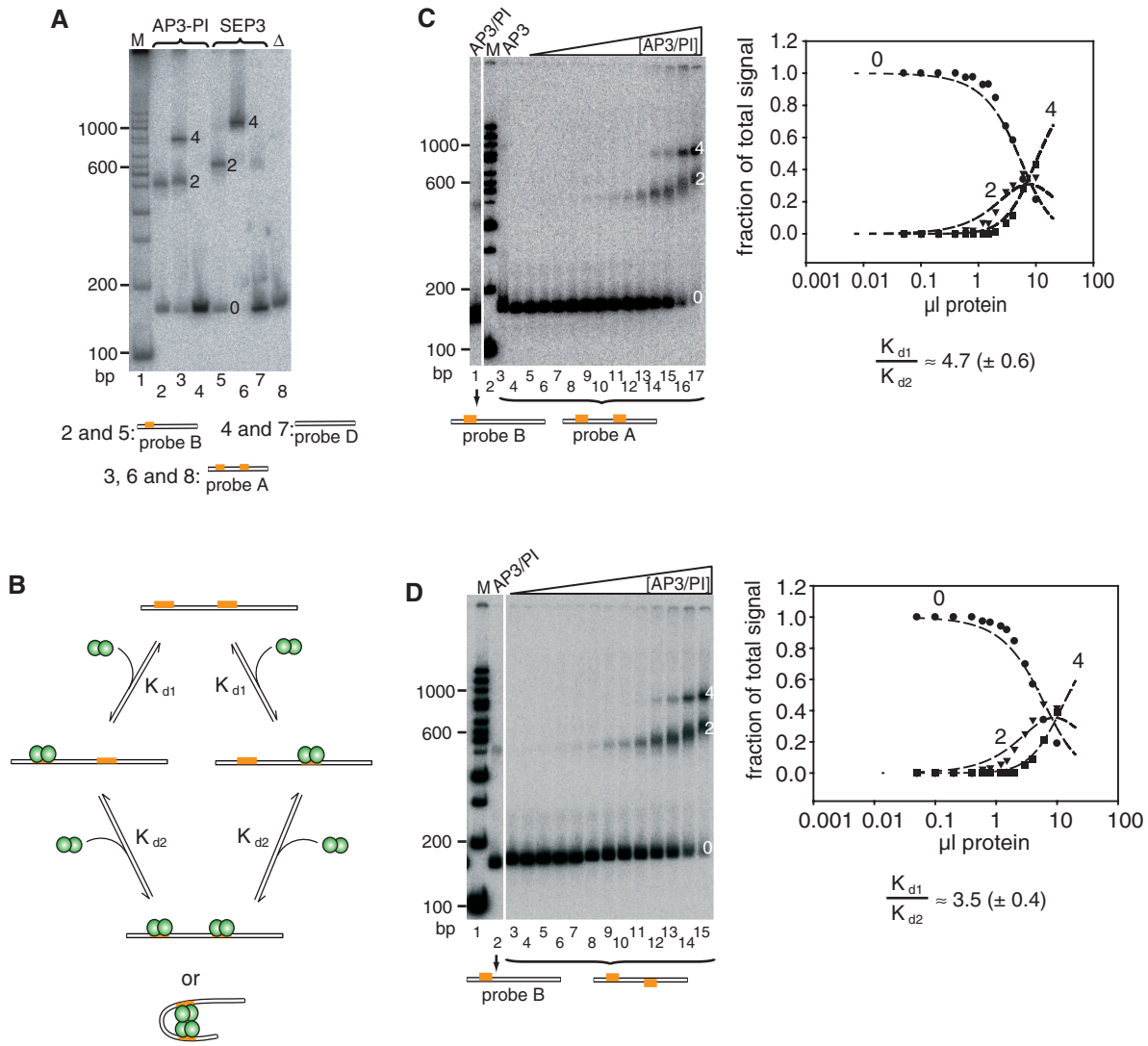

Figure 2. Analysis of binding of AP3-PI to DNA by electrophoretic mobility shift assays (EMSAs). Bands are marked with numbers ('0', '2' and '4') according to the supposed number of proteins bound to the DNA fragment. 'M' denotes marker lanes in which a radioactively labelled DNA ladder (100-bp DNA ladder, NEB) was applied. Below the gel pictures and in (**B**), the probes applied are symbolized with icons as in Figure 1, with DNA fragments as double lines and CArG boxes as orange bars. (**A**) Comparison of electrophoretic mobilities of SEP3-DNA and AP3-PI-DNA complexes. Two microlitres of *in vitro* translated AP3-PI or 0.5 µl of *in vitro* translated SEP3 was incubated with probe B (lanes 2 and 5), or probe A (lanes 3 and 6). Probe D was used to control for sequence specificity of DNA binding (lanes 4 and 7). The weak binding of SEP3 to probe D as shown in lane 7 was occasionally observed and is probably due to the presence of a CarG-box-like sequence in this probe (see Supplementary Table 2). 'Δ' denotes a negative control in which the *in vitro* translation assay was programmed only by empty pTNT vector and co-incubated with probe A (lane 8). (**B**) Proposed pathways of MADS domain protein–DNA assembly. Binding of the first protein dimer to a CArG box is characterized by the dissociation constant K_{d1}, binding of the second dimer is characterized by the dissociation constant K_{d2}. Binding of the second dimer can be independent of binding of the first dimer, or co-operative and involving DNA looping. (**C**, **D**) Examples of EMSAs used to determine co-operativity of DNA binding of AP3-PI proteins. Increasing amounts of AP3-PI (equivalent to 0.05; 0.1; 0.2; 0.4; 0.6; 0.8; 1.2; 1.5; 2; 3; 4; 6; 10 µl of *in vitro* co-translated protein) were added to a DNA probe carrying two CArG boxes. For size comparison, an AP3-PI dimer (2 µl of *in vitro* translated protein) bound to probe B is shown as indicated. Quantitative analysis showing the fractional saturation of the different bands (circles: free DNA; triangles: one dimer bound; squares: two dimers or one tetramer bound) is shown beneath each gel picture. K_{d1}/K_{d2} ratios are shown below the graphs. K_{d1}/K_{d2} ratios represent the mean of at least three experiments; standard errors are given in brackets. (C) Probe A (carrying two *AG*-derived CArG boxes spaced by six helical turns) was used. AP3 (10 µl of *in vitro* translated protein), by itself is not expected to bind to DNA and thus was used as a negative control. In lane 4 DNA without protein was applied. (D) Spacing between the *AG*-derived CArG boxes was 6.5 helical turns.

in a band of the same mobility when AP3-PI was present, but not without AP3-PI (Figure 3B, compare lanes 3, 8 and 9). This suggests that this band contains DNA fragments to which both, SEP3 dimers and AP3-PI dimers, are bound. It may also include DNA fragments to which two dimers of AP3-PI have been bound, because these have almost the same electrophoretic mobility. They can represent only a minor fraction of all complexes, however, because with the protein amounts used such complexes form quite inefficiently compared to complexes containing

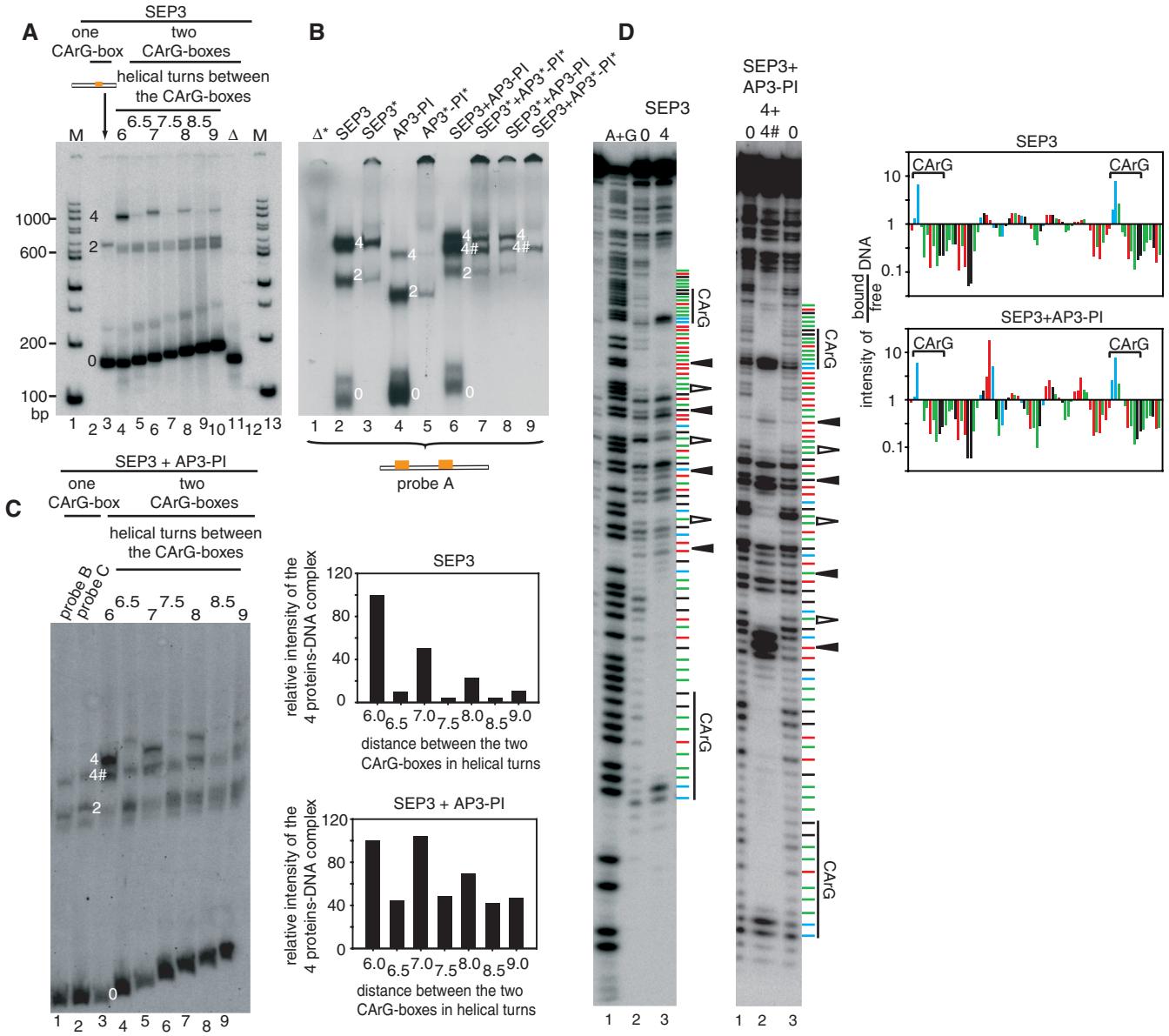

Figure 3. Formation of SEP3-SEP3/AP3-PI complexes. As in Figure 2, bands are marked with numbers ('0', '2' and '4') according to the supposed number of proteins bound to the DNA fragment. '4#' denotes bands supposed to contain SEP3 and AP3-PI bound to the same DNA fragment. 'M' denotes marker lanes. DNA probes are symbolized with icons as in Figure 1. (**A**) Formation of SEP3 homotetramers. Probes in which the phasing between two *AG*-derived CArG boxes varied as noted aboved the gel were co-incubated with 0.4 µl of *in vitro* translated SEP3. A SEP3 dimer bound to probe C is shown for comparison in lane 3. 'Δ' denotes a negative control in which the *in vitro* translation assay was programmed only by empty pTNT vector and co-incubated with probe A. (**B**) EMSA experiment in which SEP3 and/or AP3-PI were incubated with probe A. Proteins that were radioactively labelled with ^{35}S methionine during the *in vitro* translation are marked by asterisks. When at least one of the proteins was labelled, unlabelled DNA fragments were used, otherwise the DNA-fragment was labelled. The binding cocktail contained 1.5 µl of *in vitro* translated protein or, in cases where SEP3 was incubated with AP3-PI, 1.5 µl of each of the two *in vitro* translations. All labelled or unlabelled proteins of the same type were taken from the same *in vitro* translation reaction and thus had the same activity. 'Δ' denotes a negative control in which empty pSPUTK vector was applied (*in vitro* translated with ^{35}S methionine and incubated with unlabelled DNA). (**C**) Phase dependence of the formation of a DNA bound SEP3-SEP3/AP3-PI complex. The binding cocktail contained 0.5 µl of *in vitro* translated protein. SEP3, AP3 and PI were co-translated in a single reaction. Signals resulting from complexes bound to probes B and C are shown in the leftmost lanes. The other probes contained two copies of the *AG*-derived CArG box (probe A in lane 3). Phasing between the CArG boxes was varied as noted aboved the gel. On the right of the gel picture, quantitative analysis of homo- and heterotetramer formation is shown. Fractional saturation of the signal intensity caused by the different tetramers is expressed as percentage of the fractional saturation of the homo- or heterotetramers bound to probe A (lane 3). (**D**) DNase I footprint assays. SEP3 or SEP3 + AP3-PI was incubated with probe A. SEP3 and AP3-PI were separately translated and equal amounts were mixed. SEP3 preparations used in the left and right part of the figure were from different *in vitro* translation assays but the same results were obtained with aliquots. '0', '4' and '4#' indicate protection patterns obtained for free DNA ('0') and complexes '4' and '4#' extracted from an EMSA gel. As complexes '4' and '4#' migrate closely together, it was not possible to excise them separately. To obtain the 'free DNA' pattern, the DNA probe was incubated with an *in vitro* translation reaction that contained empty pTNT vector. An A + G sequencing reaction of the DNA probe is shown for comparison. Sequence of the DNA is depicted on the right (blue = cytosine, red = thymine, green = adenine, black = guanine); the position of the CArG boxes is indicated. Open and filled arrowheads point towards sites of diminished and enhanced DNase I sensitivity, respectively, after binding of protein. Beneath the gel picture, quantitative analysis of the DNAse I footprint assays shows the change of sensitivity to DNase I digestion after protein binding in single base pair-steps, using free DNA as a reference. Values were corrected for differences in DNA loading by using invariable internal bands as a reference and represent the mean of two experiments.

SEP3 tetramers (Figure 3B, compare lanes 2 with 4 and 3 with 5). With this experiment it cannot be determined, however, whether the dimeric proteins bound independently to the two CArG boxes, or whether tetrameric complexes were bound to DNA. As noted above, formation of tetrameric complexes involving DNA looping can be recognized by stereospecificity of binding. We thus used DNA probes in which the spacing between the two CArG boxes varied between six and nine helical turns in increments of half helical turns to study stereospecificity in binding of SEP3 and AP3-PI. Indeed, formation of the complexes containing four proteins (Figure 3C, bands 4 and 4#) periodically decreased when the CArG boxes were separated by a non-integral number of helical turns. This is typical for protein complexes binding to two separated DNA sites by looping the intervening region (44,45). Since DNA fragments bound by two AP3-PI heterodimers constitute only a minor fraction of band 4# (Figure 3B), and since constitution of respective complexes is almost insensitive to the phasing of the DNA binding sites (CArG boxes) (Figure 2C and D; Figure 5B), we conclude that in this case constitution of DNA bound tetrameric SEP3-SEP3/AP3-PI complexes mainly contributes to the phase dependent complex formation.

Interestingly, a band of similar mobility to that containing SEP3-SEP3/AP3-PI complexes was also observed when the respective proteins were incubated with probes containing only one CArG box (Figure 3C, lanes 1 and 2; for further discussion, see below).

To further study whether SEP3, AP3 and PI constitute a tetrameric SEP3-SEP3/AP3-PI complex that loops DNA rather than individually bound dimers, we performed DNase I footprint analyses as described (30). DNase I preferentially cuts in widened minor grooves and thus is a sensitive detector of structural changes in DNA. Importantly, in our assay we separated after DNase I digestion protein–DNA complexes from free DNA by gel electrophoresis, so that we could analyse protein bound and free DNA independently (46).

When binding of SEP3 to a DNA probe containing two CArG boxes (probe A) was investigated in DNase I footprint assays, not only protection of the region around the CArG boxes was detected, but the intervening region between the CArG boxes showed a characteristic pattern of sites with enhanced and diminished DNase I sensitivity (Figure 3D and ref. 30). Sites of similar differential sensitivity are spaced by ~10 bp; they thus all come to lie on one side of the DNA helix, yielding a pattern typical for looped DNA (43,44).

When AP3-PI was added to SEP3 in the same kind of assay, some of the differences for sites with enhanced and diminished sensitivity appeared to be increased (Figure 3D). As protein–DNA complexes were separated from free DNA prior to analysis of DNA on sequencing gels, it appears likely that DNA loops induced by SEP3-SEP3/AP3-PI complexes are more stable than loops induced by SEP3 homotetramers alone and thus sites of enhanced and diminished sensitivity are more easily detected for SEP3-SEP3/AP3-PI-DNA complexes.

SEP3-SEP3/AP3-PI complexes form on suboptimal CArG boxes and depend on the K3 subdomain of SEP3

In case of strong co-operativity, a protein dimer bound to a strong binding site may facilitate binding of another dimer to a neighbouring weak binding site (47,48). We therefore tested binding of SEP3, AP3-PI or SEP3 + AP3-PI to several probes containing CArG boxes and/or CArG box-like sequences. Sequences of the probes used are listed in Supplementary Table 2. As mentioned above, probe A contains two copies of a CArG box derived from the regulatory intron of *AG* that are spaced by six helical turns (63 bp) and perfectly match the canonical $CC(A/T)_6GG$ motif. Probe E carries the CArG box from the regulatory intron of *AG* and a sequence derived from the promoter of *GLO*. This sequence carries a CArG box-like motif that has two mismatches to the canonical $CC(A/T)_6GG$ motif (sequence is 5′-CCA**C**AATAG**A**-3′, mismatches are in bold) and that was detected to be bound only weakly by *Antirrhinum* MADS domain proteins (12,32). When using a DNA fragment carrying no perfect CArG box but the the CArG box-like sequence derived from the *GLO* promoter (probe F), we could not reproducibly detect binding activity of SEP3, AP3-PI or SEP3 together with AP3-PI under our experimental conditions, although a weak binding was occasionally observed (Figure 4A, lane 4). Also, when SEP3 and AP3-PI were incubated separately with probe E, the majority of protein was only able to bind to one site on the DNA, very likely the 'perfect', *AG*-derived binding site, as concluded from size comparisons with complexes formed when probe B (that carries only the *AG*-derived CArG box) was used (Figure 4A, compare lanes 11 and 18; 12 and 19). In addition, a faint band of low mobility was observed when SEP3 was incubated with probe E (Figure 4A, lane 18). This band was particularly evident at higher protein concentrations (Figure 4B, lanes 1 to 6 and Supplementary Figure 1) and likely represents simultaneous binding of SEP3 to the *AG*-derived CArG box and to the CArG box like sequence derived from the *GLO* promoter or another CArG box like sequence on the DNA-probe. If, however, SEP3 was incubated together with AP3-PI and probe E, formation of a complex of low mobility was strongly enhanced, suggesting that a complex of SEP3-SEP3/AP3-PI binds co-operatively to probe E (Figure 4A, lane 22). Increasing the protein concentration of either AP3-PI or SEP3 until at least 50% of probe E was bound did mainly yield dimeric complexes (Figure 4B, lanes 1 to 6 and 7 to 12), whereas a complex of lower mobility was clearly detectable even when much lower concentrations of SEP3 together with AP3-PI were co-incubated with probe E (Figure 4B, lanes 13 to 17). This clearly demonstrates that a SEP3-SEP3/AP3-PI complex indeed forms preferentially over other possible combinations.

Notably, a complex of low mobility also formed when SEP3 together with AP3 and PI were incubated with probe B or C (Figure 3C, lanes 1 and 2, Figure 4A, lane 15 and Supplementary Figure 2). Adding increasing amounts of AP3-PI to a fixed amount of SEP3 and incubation with probe B yielded this complex, while SEP3 or

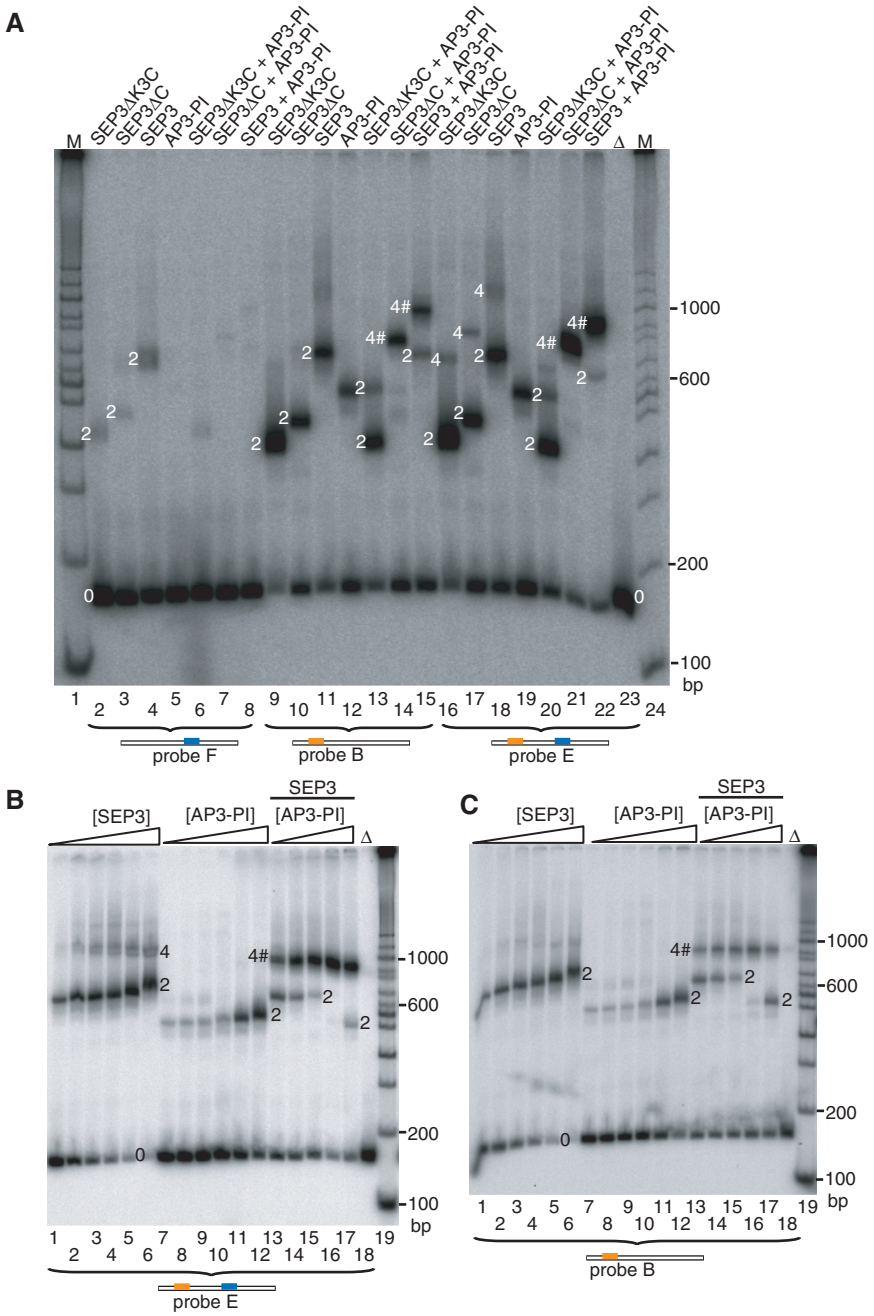

Figure 4. Binding of SEP3 and AP3-PI to DNA fragments carrying different CArG boxes. Band assignment is as in Figure 3. '4#' denotes bands supposed to contain SEP3 or SEP3ΔC and AP3-PI bound to the same DNA fragment. (**A**) Comparison of binding of SEP3, SEP3ΔC, SEP3ΔK3C, AP3-PI and combinations thereof (as noted above the gel) to probes F, B and E. Probes used are shown schematically below the gel using icons as in Figure 1. The binding cocktail contained 2 µl of *in vitro* translated SEP3ΔK3C or AP3-PI or 1 µl of *in vitro* translated SEP3ΔC or SEP3. If co-translated AP3-PI was applied together with another protein, half of the amount of each of the respective proteins was used compared to the lanes where they were applied separately. All proteins of the same type were taken from the same *in vitro* translation reaction and thus had the same activity. (**B**) Binding of SEP3 and AP3-PI to probe E. Increasing amounts of SEP3 (lanes 1 to 6) or AP3-PI (lanes 7 to 12) were incubated with probe E. Protein amounts used were equivalent to 0.1; 0.25; 0.5; 1; 2; and 4 µl of *in vitro* translated protein. In lanes 13 to 17, increasing amounts of AP3-PI (equivalent to 0.1; 0.25; 0.5; 1 and 2 µl) were added to 0.25 µl of *in vitro* translated SEP3 and incubated with probe E. Four microlitres of an *in vitro* translation assay containing empty pTNT and probe E was used as a negative control (lane 18). (**C**) Binding of SEP3 and AP3-PI to probe B. Protein amounts used and the order of loading is as in (B) but probe B instead of probe E was used. In (B) and (C) proteins of the same type were taken from the same *in vitro* translation and thus had the same activity.

AP3-PI alone generated almost only dimeric complexes at the protein concentrations being used here (Figure 4C). This corroborates the interpretation that it is a SEP3-SEP3/AP3-PI heterotetramer bound to DNA.

However, when using a short oligonucleotide (51 bp) encoding the *AG*-derived CArG box instead of the usually used longer DNA fragments, a SEP3-SEP3/AP3-PI complex was not detected under our experimental conditions

(Supplementary Figure 2). These data indicate that at the protein concentrations used here, SEP3-SEP3/AP3-PI complexes do not form tetramers bound to one CArG box only. Thus binding of tetramers probably requires simultaneously binding to one CArG box and to another DNA site with which interaction may be weak but sufficient to form a complex if a 'perfect' CArG box is in vicinity. The base composition of this second site remains unclear. Though in addition to a perfect CArG box probe C also carries a CArG box-like sequence (5′-CGATAAAAC G-3′), no second sequence that has less than three mismatches to the canonical CArG motif [5′-CC(A/T)$_6$ GG-3′] was detected in probe B (Supplementary Table 2).

To study which domains contribute to tetramer formation, we tested whether two truncated versions of SEP3, SEP3ΔC and SEP3ΔK3C, are still capable of forming heterotetramers together with AP3-PI. SEP3ΔC lacks only the C terminal domain while SEP3ΔK3C lacks both, the K3 subdomain and the C terminal domain. Both of the truncated versions were co-incubated with probe B and E and, similarly to the SEP3 full-length versions, both proteins mainly bound to one site on these DNA fragments, very likely the *AG*-derived CArG box (Figure 4A, consider lanes 9 and 16; 10 and 17). However, co-incubation of SEP3ΔC with AP3-PI and probe E yielded an intense band of low mobility (band 4#) indicative of a DNA-bound SEP3ΔC-SEP3ΔC/AP3-PI heterotetramer (Figure 4A, lane 21). In contrast, the incubation of SEP3ΔK3C with AP3-PI resulted in the detection of protein–DNA complexes containing either AP3-PI or SEP3ΔK3C protein dimers, while a complex of lower mobility indicative of a DNA bound tetramer was hardly detectable (Figure 4A, lane 20, where the dimeric complexes are marked with '2'). Also similarly to SEP3, co-incubation of SEP3ΔC with AP3-PI and probe B yielded a complex of low mobility (Figure 4A, lane14, band 4#), indicating that a tetramer composed of SEP3ΔC and AP3-PI was bound to probe B. In contrast, co-incubation of SEP3ΔK3C with AP3-PI and probe B only resulted in formation of complexes with an electrophoretic mobility very similar to DNA-bound SEP3ΔK3C and AP3-PI dimers (Figure 4A, compare lanes 9 and 12 with lane 13), indicating that either SEP3ΔK3C dimers or AP3-PI dimers were bound to probe B and that tetrameric complexes were not formed.

Since with the protein amounts used SEP3ΔK3C bound more of the DNA than SEP3 did (Figure 4A, compare lanes 9 and 11), lack of formation of a DNA-bound tetrameric complex when SEP3ΔK3C (Figure 4A, lanes 13 and 20) rather than SEP3 (Figure 4A, lanes 15 and 22) was co-incubated with AP3-PI, was not due to insufficient amounts of SEP3ΔK3C in the respective samples.

Taken together, our data indicate that the K3 subdomain is of importance for the formation of heterotetrameric SEP3-SEP3/AP3-PI complexes, at least in the absence of the C terminal domain.

The K3 subdomain of SEP3 is sufficient for tetramer formation in the sequence context of AP3 and PI

To better understand the relevance of the K3 subdomain for DNA-bound tetramer formation, two chimeric constructs, termed 'AP3∼SEP3' and 'PI∼SEP3', were generated, consisting of the MADS, I, K1 and K2 regions from AP3 or PI, respectively, followed by the K3 domain from SEP3. In electrophoretic mobility shift assays we were not able to detect DNA binding of the resulting chimeric AP3∼SEP3 and PI∼SEP3 proteins as homodimers, indicating that they still possess the dimerization specificity (that is, obligate heterodimerization) of wild-type AP3 and PI (Figure 5A). However, when AP3∼SEP3 and PI∼SEP3 were incubated together, they did not only show DNA-binding activity to one (Figure 5A, lane 8) and two CArG-boxes (Figure 5A, lane 14), but, similar to SEP3, also a strong stereospecificity in binding to DNA fragments containing two CArG boxes (Figure 5B). This is in contrast to the wild-type AP3-PI proteins that showed only weak stereospecificity in DNA binding (Figures 2C and D; Figure 5B). These data indicate that the K3 domain of SEP3 is, in the context of AP3 and PI, sufficient to mediate tetramer formation.

A model for floral quartets

Our view on the structure of a floral quartet is shown in Figure 6. In this model, the change in susceptibility of DNA to DNase I digestion after SEP3-SEP3/AP3-PI binding to DNA was used to modify the roll angles of a standard B DNA (Figure 6A). The CArG boxes were then replaced by the bent CArG boxes present in the crystallized CArG–SRF complex (38) and the structure of the crystallized MADS domain of the human SRF (38) was plotted on this DNA to infer the position of the protein dimers (Figure 6B). The limitations of such a model notwithstanding, the resulting arrangement is similar to other cases of protein-induced DNA loops (49) and might thus not be far-fetched.

DISCUSSION

Evidence for a DNA bound SEP3-SEP3/AP3-PI tetramer

The 'floral quartet model' predicts that different combinations of tetrameric complexes of floral homeotic proteins bind to two *cis*-regulatory elements on DNA; SEP proteins are considered being important (maybe even essential) constituents of these complexes that enable floral quartet formation and provide transcriptional activation domains (2,8,9,13,30). Genetic data show that the ectopic expression of *SEP3*, *AP3* and *PI* is sufficient to convert lateral organ primordia that would otherwise develop into rosette leaves into petal primordia (13). In conjunction with pull-down and yeast three-hybrid experiments showing that SEP3, AP3 and PI interact physically this was taken as evidence that a complex containing SEP3, AP3 and PI is able to specify petal identity (13). However, it has essentially remained unknown whether and how such a complex indeed assembles on DNA, and whether it assembles *in planta*. Most importantly, other models for the interaction of floral homeotic proteins with the DNA of target genes not involving floral quartet formation remained plausible alternative scenarios that fit available data (17). For example, ternary or quaternary

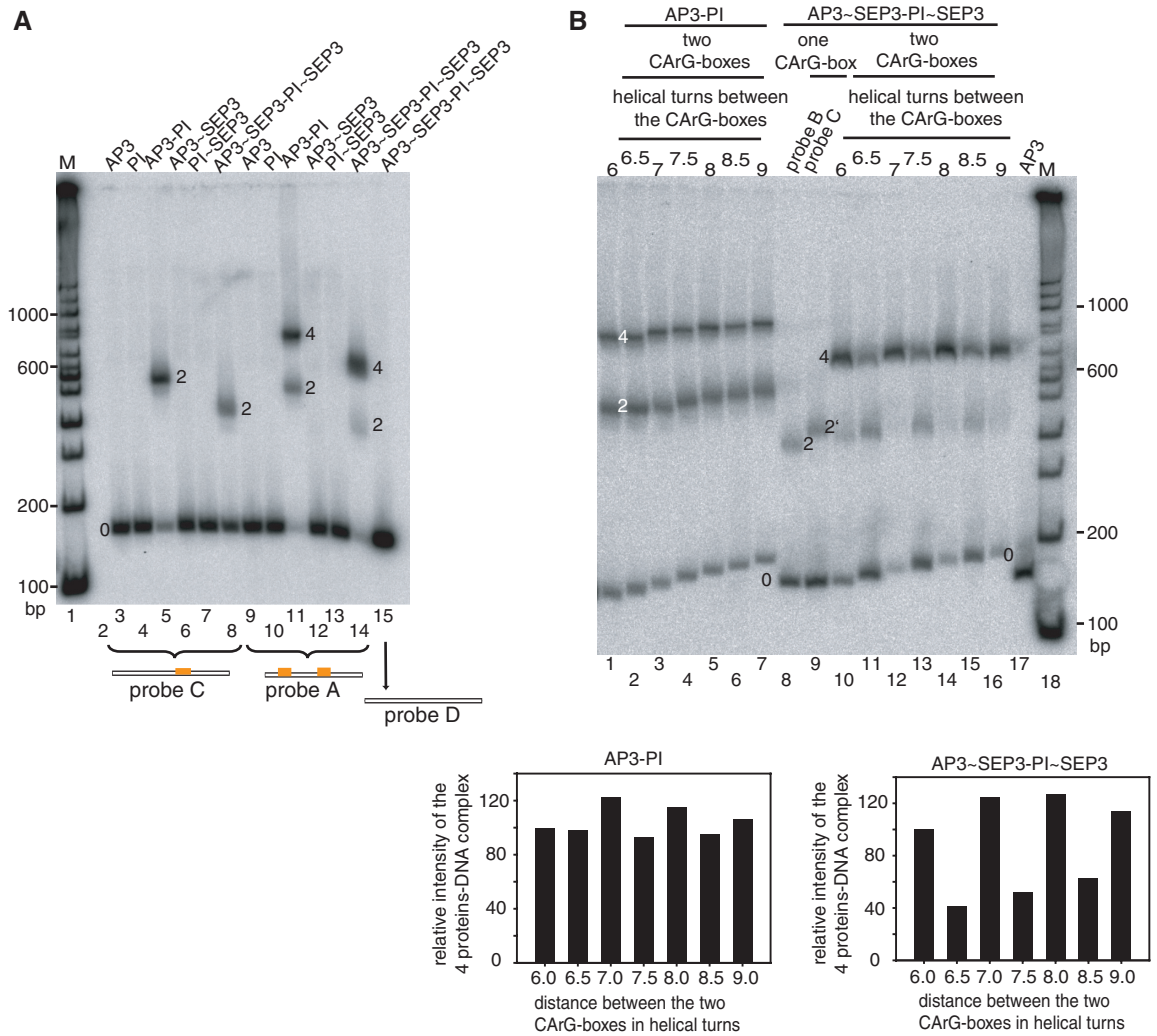

Figure 5. DNA binding of chimeric AP3∼SEP3-PI∼SEP3 complexes. Band assignment is as in Figure 3 (**A**) DNA-binding activity of individually translated AP3, PI, AP3∼SEP3 and PI∼SEP3 was tested in comparison to cotranslated AP3-PI and AP3∼SEP3-PI∼SEP3 proteins. Two microlitres of *in vitro* translated proteins were used. In lanes 3 to 8, probe C was used, in lanes 9 to 14, probe A was applied. Binding of AP3∼SEP3-PI∼SEP3 to probe D was used to test for sequence-specificity of DNA binding (lane 15). (**B**) Phase dependence of the formation of DNA bound AP3-PI and AP3∼SEP3-PI∼SEP3 complexes. The binding cocktail contained 1 µl of *in vitro* translated protein. Signals resulting from AP3∼SEP3-PI∼SEP3 complexes bound to probes B and C are shown in lanes 8 and 9, respectively. As the proteins are able to bend the DNA, the different positioning of the CArG box on the fragment results in a difference in migration of the complexes (2 and 2′). As in Figure 3C, the other probes contained two copies of the *AG*-derived CArG box (probe A in lanes 1 and 10) and phasing between the CArG boxes was varied as noted above the gel. AP3, that alone is not expected to bind to DNA was used as a negative control and co-incubated with probe A (lane 17). Below the gel picture, quantitative analysis of the complexes consisting of four proteins bound to DNA is shown. Fractional saturation of the signal intensity caused by these complexes is expressed as percentage of the fractional saturation of the respective complexes bound to probe A.

complexes of floral homeotic proteins binding to only one *cis*-regulatory DNA element may control the activity of target genes (17).

Our data indicate that the class B floral homeotic proteins AP3 and PI bind to DNA in a co-operative way only very weakly, at best, even when two suitable binding sites (CArG boxes) are present on the DNA in a favourable distance and phasing (Figure 2C and Figure 5B), and do hence not form tetrameric complexes easily. However, AP3 and PI readily bind to DNA in a co-operative way together with SEP3 (Figures 3C and 4A). Our data suggest that this co-operative binding involves DNA looping (Figure 3D), is stereospecific (Figure 3C) and largely depends on the subdomain K3 of SEP3 (Figure 4A), a domain that is supposed to be of importance for protein–protein interactions (20). It therefore appears plausible that this co-operative binding is mediated by a direct contact between an AP3-PI heterodimer and a SEP3-SEP3 homodimer. We thus conclude that DNA bound SEP3-SEP3/AP3-PI heterotetramers can be reconstituted *in vitro*, while complexes such as AP3-PI/AP3-PI, that involve only class B proteins, do not easily form. Furthermore, SEP3-SEP3/AP3-PI complexes also form on DNA-probes to which SEP3 homotetramers do not easily bind, indicating that heterotetramers of SEP3 and class B proteins form preferentially over SEP3 homotetramers (Figure 4). The strength of tetramer formation would therefore be in the order SEP3-SEP3/AP3-PI

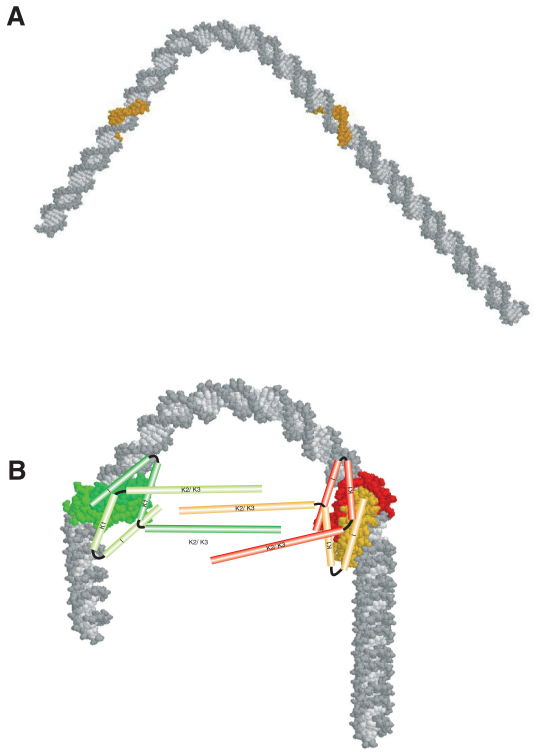

Figure 6. Model of a floral quartet. (**A**) B DNA of which roll angles have been changed according to the differences of sensitivity to DNase I digestion of SEP3-SEP3/AP3-PI bound DNA versus free DNA (see 'Materials and Methods' section). The CArG boxes on one strand are shown in orange. (**B**) The DNA shown in (A) is modified so that the MADS domain structure of SRF can be plotted on it to infer the relative orientation of the proteins. The original CArG boxes have been replaced by the bent CArG boxes from the SRF–CArG complex (see 'Materials and Methods' section). Possible positions of the I and K domains are shown schematically. The C terminus is omitted for simplicity.

heterotetramers > SEP3 homotetramers > AP3-PI/AP3-PI heterotetramers. This interpretation is supported by the notion that stereospecificity in binding of two AP3-PI dimers is very weak (Figure 5B), whereas that for two SEP3 dimers is clearly stronger (Figure 3A and C). Formation of SEP3-SEP3/AP3-PI complexes, on the other hand, was often observed to be less stereospecific than that of SEP3 homotetramers (Figure 3C), probably because stability of SEP3-SEP3/AP3-PI tetramers is so high that it can partly compensate for suboptimal orientation of the CArG boxes.

Taken together, these data corroborate predictions of the floral quartet model about the combinatorial interaction and DNA binding of floral homeotic proteins. Specifically, our *in vitro* data make it appear likely that petal identity can indeed be specified *in planta* by a complex involving SEP3-SEP3/AP3-PI heterotetramers bound to target gene DNA containing two CArG boxes.

However, according to both, the ABC model and the floral quartet model, also the class A floral homeotic protein AP1 is involved in petal development and thus has been predicted to be part of a respective complex (7,8). On the other hand, it has been repeatedly argued that the function of AP1 in specifying sepal and petal identity can be seen as a concomitant effect of its ancestral function in floral meristem specification (15,16). This is consistent with both the phenotype of strong *ap1* mutants, in which petals are not homeotically transformed into other organs but missing (and secondary flowers develop in the axils of first whorl organs); and the fact that *AP1* is not strictly required for petal formation (50,51). But nevertheless, also the ectopic expression of AP1 together with AP3 and PI leads to the conversion of organ primordia that would normally develop leaves into petal primorida (13). One possibility to interpret these data is that AP1 [whose mRNA is detectable very early in flower development at stage 1 (52,53)] or a protein complex containing AP1 acts upstream of *SEP3* and activates expression of *SEP3* [which is expressed during flower development from stage 2 onwards (54)]. In turn, SEP3-SEP3/AP3-PI and/or SEP3-AP1/AP3-PI complexes may form and function in specifying petal development in a partly redundant fashion. Consistent with this idea, *ap1* mutant plants develop petals if SEP3 is constitutively expressed under control of the Cauliflower Mosaic Virus (CaMV) 35S promoter. However, the fact that the *AP1*-related gene *CAULIFLOWER* (*CAL*) is required for petal formation in *ap1 35S::SEP3* plants (51) suggests that *in vivo*, different complexes containing AP1, CAL or SEP proteins and AP3-PI heterodimers may form and accomplish partly overlapping functions. Possibly, only isolation of the respective floral homeotic protein complexes from floral organs will reveal which DNA-bound tetrameric complexes form *in vivo*. It further remains an important goal for future research to study whether other DNA-bound complexes predicted by the floral quartet model (such as SEP3-AG/AP3-PI complexes for specifying stamen identity or SEP3-AG/SEP3-AG complexes for specifying carpel identity) indeed form and function *in planta*. Nevertheless, we think that the main characteristics of the protein–DNA complexes characterized in this work provide general clues as to how functional floral homeotic MADS domain protein complexes are formed and how they recognize their target genes.

The formation of distinct protein complexes during flower development

MADS domain proteins are involved, among other things, in specifying floral meristem identity, in determining floral organ identity, and also in controlling the development of substructures of floral organs such as ovules within carpels and the endothelium within ovules (2,3,55). SEP3 is believed to be important during all these steps of flower development. Thus, it has been proposed that SEP proteins and specifically SEP3 are major constituents of complexes of MADS domain proteins, and that they interact with different other MADS domain proteins, depending on their temporal order of availability (51). For example, tetramers composed of SEP3 and/or AP1 may, together with LEAFY, activate *AP3, PI* and *AG* (51). Afterwards, AG and/or AP3 and PI may interact with SEP proteins to form complexes that promote floral organ identity. Later in development, complexes important for ovule

development containing class D proteins and again SEP proteins might be formed (51). In case of co-expressed proteins, this scenario would be facilitated if at each step the newly expressed MADS domain proteins interact more favourably with SEP proteins than the previous ones. Our results suggest that SEP3-SEP3/AP3-PI complexes form preferentially over SEP3 homotetramers. This would be in accordance with a role of SEP3 homotetramers early during flower development and of SEP3-SEP3/AP3-PI heterotetramers at later stages when organ identity has to be specified.

As mentioned above, different MADS domain proteins and protein complexes specifically control different floral developmental processes. It is generally assumed that the distinct functions of the different protein complexes are brought about by the differential regulation of target genes. How this target gene specificity is achieved is largely unclear, however. Initially, it was assumed that different dimers of MADS domain proteins bind to different CArG box sequences. However, although some differences in DNA-binding specificity between, for example, homodimers of AP1 and AG and heterodimers of AP3 and PI have been observed, evidence has been presented suggesting that these differences can not explain target gene specificity satisfactorily (26,39,56). For example, substituting the N-terminal half of the MADS domain of AP3 with the corresponding region of MEF2A results in a chimeric protein that shows (as a heterodimer with PI) *in vitro* DNA-binding characteristics that were substantially different form those of the wild-type AP3-PI heterodimer. Nevertheless, this chimeric protein was able to rescue *ap3* mutant phenotypes (56). Furthermore, domain-swapping experiments indicated that the functional specificity of AP3 and PI resides in the I and K domains, i.e. in regions known to be important for protein–protein interactions, but not in the DNA binding MADS domain (26). Based on these data it was suggested that target gene specificity of MADS domain proteins is achieved by interactions with additional cofactors (26,39,56). So far, evidence for the existence of such cofactors is sparse, however (ref. 10 and references cited therein). As mentioned above, SEP3-SEP3/AP3-PI heterotetramers seem to form preferentially over SEP3 homotetramers. We suggest that this is accomplished because binding affinity between SEP3-SEP3 homodimers and AP3-PI heterodimers exceeds that between two SEP3 homodimers. Importantly, this higher affinity between the dimers leads to binding of *cis*-regulatory DNA elements that are not or only weakly bound by SEP3 homotetramers (Figure 4). In general, SEP3-SEP3/AP3-PI heterotetramers might recognize a broader spectrum of *cis*-regulatory sequences and hence control more target genes than SEP3 homotetramers. This is consistent with the supposed role of SEP3 homotetramers in activating the floral homeotic genes and the role of SEP3-SEP3/AP3-PI complexes in maintaining expression of *SEP3*, *AP3* and *PI* but also in activating additional genes that are necessary for petal development.

Notably, this putative difference in target gene specificity could in principle be brought about only by the differential stability of the tetramers; different binding affinities of AP3-PI and SEP3-SEP3 dimers to the same CArG boxes may not be required. It is thus conceivable that part of the target gene specificity of floral homeotic proteins is neither regulated at the level of individual dimers nor by additional cofactors but rather at the level of tetramer formation (or, in other words, one dimer of MADS domain proteins serves as cofactors for another dimer to determine target gene specificity). It is currently unclear, however, to what extent target gene specificity of floral homeotic proteins really depends on formation and stability of multimeric protein complexes. Flower development is presumed to be regulated by several different tetrameric complexes of MADS domain proteins; target gene specificity might, among other things, well be achieved by a combination of DNA sequence specificity of individual proteins, protein complex stability and synergistic (co-operative) molecular effects at the respective target gene loci.

Role of the K3 subdomain in the formation of floral-quartet-like complexes

As shown here, the subdomain K3 of SEP3 is important for the formation of DNA-bound SEP3-SEP3/AP3-PI complexes, at least in the absence of the C terminal domain (Figure 4A). This indicates that the K3 subdomain plays an important role in co-operative binding of floral homeotic proteins. Deletion of the C terminal domain had no substantial effect on higher-order complex formation. This suggests that at least in case of the proteins studied here, the C terminal domain does not participate in tetramer formation, although we cannot exclude the possibility that the C terminal domain plays a redundant role in tetramerization that would only be uncovered by an internal deletion of the K3 subdomain.

Like the wild-type AP3 and PI proteins, but unlike SEP3, chimeric AP3∼SEP3 and PI∼SEP3 proteins (containing the MADS to K2 region of AP3 or PI and the K3 region of SEP3) were only as heterodimers capable of sequence-specific DNA binding, but not as homodimers, indicating that the chimeric proteins retained the dimerization capabilities of AP3 and PI (Figure 5A). This is in line with previous deletion analyses which revealed that the C terminus and at least one-thirds of the K domain is dispensable for dimerization of class B floral homeotic proteins (39,57). However, unlike AP3-PI, but similar to SEP3, strong stereospecificity in binding to fragments containing two CArG boxes was observed for AP3∼SEP3-PI∼SEP3 (Figure 5B). These results suggest that in the context of a MADS domain protein, subdomain K3 of SEP3 is sufficient to mediate tetramerization, although it can not be ruled out at the moment that the observed stereospecificity is due to the deletion of the C terminal domain in the AP3∼SEP3 and PI∼SEP3 proteins. This could be examined in future experiments by testing C terminal deleted AP3 and PI proteins on their ability to bind stereospecific to DNA.

Despite these findings it seems quite likely that amino acid residues outside K3 also participate in tetramer formation. It has been shown, for example, that residues in the subdomain K2 of PI are important for mediating the

PI/SEP3 interaction that is supposed to take place in SEP3-SEP3/AP3-PI tetramers (19). Given the high degree of sequence similarity between floral homeotic MADS domain proteins, it would not come as a surprise to see that the K domain, and specifically subdomains K2 and K3, play a general role in the formation of tetramers of floral homeotic proteins. This would be in accordance with data suggesting that also the K3 domains of AP3 and PI, but not the C terminal domain of these proteins are required for the organ identity specification *in planta* (58). Therefore, it will be quite revealing to study the biochemical and structural properties of these domains both in a developmental and an evolutionary context.

A great deal has been learnt during the last 20 years about the mechanisms by which floral homeotic genes and proteins control flower development, mainly by the use of molecular genetic methods. We predict, however, that for learning more details about this process, methods of molecular biophysics and biochemistry, like those used here, will become more and more important. An even deeper understanding of floral homeotic protein function at the molecular level may also depend on a characterization of the way in which MADS domain multimeric complexes interact with other components of the transcriptional machinery during activation or repression of target genes. Beyond that, it is clear that a comprehensive understanding of flower development can only be achieved if we understand the underlying molecular interactions in a quantitative way. This may not only require studies on the purification and thorough biochemical characterization of the proteins and protein complexes being involved, but also a systems biology approach that integrates these data in models that make testable predictions.

SUPPLEMENTARY DATA

Supplementary Data are available at NAR Online.

ACKNOWLEDGEMENTS

The excellent technical assistance of Jana Hrtoňová and Ulrike Wrazidlo is gratefully acknowledged. We are also grateful to Markus Ritz for help with data analysis and to Gerhard Steger (University of Düsseldorf) and Thomas P. Jack (Dartmouth College, Hanover) for helpful comments on an earlier version of this manuscript. We thank the group of Jürgen Kroymann (Max Planck Institue for Chemical Ecology, Jena) for support with the phosphorimager analyses and Domenica Schnabelrauch (Max Planck Institute for Chemical Ecology, Jena) for all her sequencing efforts. We are grateful to Andrea Härter for critical reading the manuscript. Many thanks also to the Friedrich Schiller University Jena for general support. Both authors wish to express their gratefulness to Sabine Schein for navigating them through the storms of daily working life.

FUNDING

A fellowship of the Studienstiftung des deutschen Volkes (to R.M.). Funding for open access charge: Friedrich Schiller University.

Conflict of interest statement. None declared.

REFERENCES

1. Sablowski,R. (2007) Flowering and determinacy in Arabidopsis. *J. Exp. Bot.*, **58**, 899–907.
2. Krizek,B.A. and Fletcher,J.C. (2005) Molecular mechanisms of flower development: an armchair guide. *Nat. Rev. Genet.*, **6**, 688–698.
3. Jack,T. (2004) Molecular and genetic mechanisms of floral control. *Plant Cell*, **16**, S1–S17.
4. Zahn,L.M., Feng,B.M. and Ma,H. (2006) Beyond the ABC-model: Regulation of floral homeotic genes. *Adv. Bot. Res. Incorp. Adv. Plant Patho.*, **44**, 163–207.
5. Haughn,G.W. and Somerville,C.R. (1988) Genetic control of morphogenesis in *Arabidopsis*. *Dev. Genet.*, **9**, 73–89.
6. Coen,E.S. and Meyerowitz,E.M. (1991) The war of the whorls - genetic interactions controlling flower development. *Nature*, **353**, 31–37.
7. Gustafson-Brown,C., Savidge,B. and Yanofsky,M.F. (1994) Regulation of the *Arabidopsis* floral homeotic gene *APETALA1*. *Cell*, **76**, 131–143.
8. Theißen,G. (2001) Development of floral organ identity: stories from the MADS house. *Curr. Opin. Plant Biol.*, **4**, 75–85.
9. Theißen,G. and Saedler,H. (2001) Plant biology. Floral quartets. *Nature*, **409**, 469–471.
10. Melzer,R., Kaufmann,K. and Theissen,G. (2006) Missing links: DNA-binding and target gene specificity of floral homeotic proteins. *Adv. Bot. Res. Incorp. Adv. Plant Pathol.*, **44**, 209–236.
11. de Folter,S. and Angenent,G.C. (2006) trans meets cis in MADS science. *Trends Plant Sci.*, **11**, 224–231.
12. Egea-Cortines,M., Saedler,H. and Sommer,H. (1999) Ternary complex formation between the MADS-box proteins SQUAMOSA, DEFICIENS and GLOBOSA is involved in the control of floral architecture in *Antirrhinum majus*. *EMBO J.*, **18**, 5370–5379.
13. Honma,T. and Goto,K. (2001) Complexes of MADS-box proteins are sufficient to convert leaves into floral organs. *Nature*, **409**, 525–529.
14. Pelaz,S., Tapia-Lopez,R., Alvarez-Buylla,E.R. and Yanofsky,M.F. (2001) Conversion of leaves into petals in Arabidopsis. *Curr. Biol.*, **11**, 182–184.
15. Theißen,G., Becker,A., Di Rosa,A., Kanno,A., Kim,J.T., Münster,T., Winter,K.U. and Saedler,H. (2000) A short history of MADS-box genes in plants. *Plant Mol. Biol.*, **42**, 115–149.
16. Litt,A. (2007) An evaluation of A-function: evidence from the APETALA1 and APETALA2 gene lineages. *Int. J. Plant Sci*, **168**, 73–91.
17. Jack,T. (2001) Relearning our ABCs: new twists on an old model. *Trends Plant Sci.*, **6**, 310–316.
18. Yang,Y.Z., Fanning,L. and Jack,T. (2003) The K domain mediates heterodimerization of the *Arabidopsis* floral organ identity proteins APETALA3 and PISTILLATA. *Plant J.*, **33**, 47–59.
19. Yang,Y.Z. and Jack,T. (2004) Defining subdomains of the K domain important for protein-protein interactions of plant MADS proteins. *Plant Mol. Biol.*, **55**, 45–59.
20. Kaufmann,K., Melzer,R. and Theissen,G. (2005) MIKC-type MADS-domain proteins: structural modularity, protein interactions and network evolution in land plants. *Gene*, **347**, 183–198.
21. Purugganan,M.D., Rounsley,S.D., Schmidt,R.J. and Yanofsky,M.F. (1995) Molecular evolution of flower development – diversification of the plant MADS-box regulatory gene family. *Genetics*, **140**, 345–356.
22. Theißen,G., Kim,J.T. and Saedler,H. (1996) Classification and phylogeny of the MADS-box multigene family suggest defined roles of MADS-box gene subfamilies in the morphological evolution of eukaryotes. *J. Mol. Evol.*, **43**, 484–516.
23. Ma,H., Yanofsky,M.F. and Meyerowitz,E.M. (1991) *AGL1-AGL6*, an *Arabidopsis* gene family with similarity to floral homeotic and transcription factor genes. *Gene Dev.*, **5**, 484–495.
24. Huang,H., Tudor,M., Su,T., Zhang,Y., Hu,Y. and Ma,H. (1996) DNA binding properties of two *Arabidopsis* MADS domain proteins: binding consensus and dimer formation. *Plant Cell*, **8**, 81–94.

25. Riechmann,J.L., Krizek,B.A. and Meyerowitz,E.M. (1996) Dimerization specificity of *Arabidopsis* MADS domain homeotic proteins APETALA1, APETALA3, PISTILLATA, and AGAMOUS. *Proc. Natl Acad. Sci. USA*, **93**, 4793–4798.
26. Krizek,B.A. and Meyerowitz,E.M. (1996) Mapping the protein regions responsible for the functional specificities of the Arabidopsis MADS domain organ-identity proteins. *Proc. Natl Acad. Sci. USA*, **93**, 4063–4070.
27. Lim,J., Moon,Y.H., An,G. and Jang,S.K. (2000) Two rice MADS domain proteins interact with OsMADS1. *Plant Mol. Biol.*, **44**, 513–527.
28. Cho,S.C., Jang,S.H., Chae,S.J., Chung,K.M., Moon,Y.H., An,G.H. and Jang,S.K. (1999) Analysis of the C-terminal region of *Arabidopsis thaliana* APETALA1 as a transcription activation domain. *Plant Mol. Biol.*, **40**, 419–429.
29. Tzeng,T.Y., Liu,H.C. and Yang,C.H. (2004) The C-terminal sequence of LMADS1 is essential for the formation of homodimers for B function proteins. *J. Biol. Chem.*, **279**, 10747–10755.
30. Melzer,R., Verelst,W. and Theissen,G. (2009) The class E floral homeotic protein SEPALLATA3 is sufficient to loop DNA in 'floral quartet'-like complexes in vitro. *Nucleic Acids Res.*, **37**, 144–157.
31. Kaufmann,K., Anfang,N., Saedler,H. and Theissen,G. (2005) Mutant analysis, protein-protein interactions and subcellular localization of the Arabidopsis B-sister (ABS) protein. *Mol. Genet. Genomics.*, **274**, 103–118.
32. Tröbner,W., Ramirez,L., Motte,P., Hue,I., Huijser,P., Lönnig,W.E., Saedler,H., Sommer,H. and Schwarz-Sommer,Z. (1992) *GLOBOSA* – a homeotic gene which interacts with *DEFICIENS* in the control of *Antirrhinum* floral organogenesis. *EMBO J.*, **11**, 4693–4704.
33. Senear,D.F. and Brenowitz,M. (1991) Determination of binding constants for cooperative site-specific protein-DNA interactions using the gel mobility-shift assay. *J. Biol. Chem.*, **266**, 13661–13671.
34. Steger,G. (2005) Bioinformatik. Methoden zur Vorhersage von RNA- und Proteinstruktur. Birkhäuser Verlag, Basel.
35. Lu,X.J. and Olson,W.K. (2003) 3DNA: a software package for the analysis, rebuilding and visualization of three-dimensional nucleic acid structures. *Nucleic Acids Res.*, **31**, 5108–5121.
36. Brenowitz,M., Senear,D.F., Shea,M.A. and Ackers,G.K. (1986) Quantitative DNase footprint titration: a method for studying protein-DNA interactions. *Methods Enzymol.*, **130**, 132–181.
37. Martz,E. (2002) Protein Explorer: easy yet powerful macromolecular visualization. *Trends Biochem. Sci.*, **27**, 107–109.
38. Pellegrini,L., Song,T. and Richmond,T.J. (1995) Structure of serum response factor core bound to DNA. *Nature*, **376**, 490–498.
39. Riechmann,J.L., Wang,M.Q. and Meyerowitz,E.M. (1996) DNA-binding properties of *Arabidopsis* MADS domain homeotic proteins APETALA1, APETALA3, PISTILLATA and AGAMOUS. *Nucleic Acids Res.*, **24**, 3134–3141.
40. West,A.G., Causier,B.E., Davies,B. and Sharrocks,A.D. (1998) DNA binding and dimerisation determinants of *Antirrhinum majus* MADS-box transcription factors. *Nucleic Acids Res.*, **26**, 5277–5287.
41. Guex,N. and Peitsch,M.C. (1997) SWISS-MODEL and the Swiss-PdbViewer: An environment for comparative protein modeling. *Electrophoresis*, **18**, 2714–2723.
42. Tilly,J.J., Allen,D.W. and Jack,T. (1998) The CArG boxes in the promoter of the *Arabidopsis* floral organ identity gene *APETALA3* mediate diverse regulatory effects. *Development*, **125**, 1647–1657.
43. Hochschild,A. and Ptashne,M. (1986) Cooperative binding of lambda repressors to sites separated by integral turns of the DNA helix. *Cell*, **44**, 681–687.
44. Krämer,H., Niemöller,M., Amouyal,M., Revet,B., von Wilcken-Bergmann,B. and Müller-Hill,B. (1987) lac repressor forms loops with linear DNA carrying two suitably spaced lac operators. *EMBO J.*, **6**, 1481–1491.
45. Schleif,R. (1992) DNA looping. *Annu. Rev. Biochem.*, **61**, 199–223.
46. Topol,J., Ruden,D.M. and Parker,C.S. (1985) Sequences required for in vitro transcriptional activation of a Drosophila *hsp 70* gene. *Cell*, **42**, 527–537.
47. Ackers,G.K., Shea,M.A. and Smith,F.R. (1983) Free energy coupling within macromolecules. The chemical work of ligand binding at the individual sites in co-operative systems. *J. Mol. Biol.*, **170**, 223–242.
48. Burz,D.S., Rivera-Pomar,R., Jackle,H. and Hanes,S.D. (1998) Cooperative DNA-binding by Bicoid provides a mechanism for threshold-dependent gene activation in the *Drosophila* embryo. *EMBO J.*, **17**, 5998–6009.
49. Swigon,D., Coleman,B.D. and Olson,W.K. (2006) Modeling the Lac repressor-operator assembly: the influence of DNA looping on Lac repressor conformation. *Proc. Natl Acad. Sci. USA*, **103**, 9879–9884.
50. Bowman,J.L., Alvarez,J., Weigel,D., Meyerowitz,E.M. and Smyth,D.R. (1993) Control of flower development in *Arabidopsis thaliana* by *APETALA1* and interacting genes. *Development*, **119**, 721–743.
51. Castillejo,C., Romera-Branchat,M. and Pelaz,S. (2005) A new role of the *Arabidopsis SEPALLATA3* gene revealed by its constitutive expression. *Plant J.*, **43**, 586–596.
52. Wagner,D., Sablowski,R.W.M. and Meyerowitz,E.M. (1999) Transcriptional activation of *APETALA1* by LEAFY. *Science*, **285**, 582–584.
53. Mandel,M.A., Gustafson-Brown,C., Savidge,B. and Yanofsky,M.F. (1992) Molecular characterization of the *Arabidopsis* floral homeotic gene *APETALA1*. *Nature*, **360**, 273–277.
54. Mandel,M.A. and Yanofsky,M.F. (1998) The *Arabidopsis AGL9* MADS box gene is expressed in young flower primordia. *Sex Plant Reprod.*, **11**, 22–28.
55. Scutt,C.P., Vinauger-Douard,M., Fourquin,C., Finet,C. and Dumas,C. (2006) An evolutionary perspective on the regulation of carpel development. *J. Exp. Bot.*, **57**, 2143–2152.
56. Riechmann,J.L. and Meyerowitz,E.M. (1997) Determination of floral organ identity by Arabidopsis MADS domain homeotic proteins AP1, AP3, PI, and AG is independent of their DNA-binding specificity. *Mol. Biol. Cell*, **8**, 1243–1259.
57. Zachgo,S., de Andrade Silva,E., Motte,P., Tröbner,W., Saedler,H. and Schwarz-Sommer,Z. (1995) Functional analysis of the *Antirrhinum* floral homeotic *DEFICIENS* gene in vivo and in vitro by using a temperature-sensitive mutant. *Development*, **121**, 2861–2875.
58. Piwarzyk,E., Yang,Y.Z. and Jack,T. (2007) Conserved C-terminal motifs of the Arabidopsis proteins APETALA3 and PISTILLATA are dispensable for floral organ identity function. *Plant Physiol.*, **145**, 1495–1505.